Journal of Energy Storage 174 (2026) 123040

Contents lists available at ScienceDirect

Journal of Energy Storage

journal homepage: www.elsevier.com/locate/est

Research Papers

System-level analysis of energy storage requirements for large-scale renewable integration

Teklebrhan Negash [a,f,*], Solomon A.A. [b], Fredric Ottermo [c], Erik Möllerström [c,**], Seres István [d], Farkas István [e]

[a] Doctoral School of Mechanical Engineering, Hungarian University of Agriculture and Life Sciences, Godöllö, Hungary
[b] School of Technology and Innovations, University of Vaasa, Wolffintie 34, 65200, Vaasa, Finland
[c] School of Business, Innovation and Sustainability, Halmstad University, PO Box 823, SE-301 18, Halmstad, Sweden
[d] Institute of Mathematics and Basic Science, Hungarian University of Agriculture and Life Sciences, Godöllö, Hungary.
[e] Institute of Technology, Hungarian University of Agriculture and Life Sciences, Godöllö, Hungary.
[f] Department of Mechanical Engineering, MaiNefhi College of Engineering and Technology, PO Box 12676, Asmara, Eritrea

ARTICLE INFO

Keywords:
Renewable energy integration
PV-wind mix
Diurnal storage
Seasonal storage
Penetration
Curtailment
Balancing requirement

ABSTRACT

Driven by cost reductions, improved performance, and advancements in smart technologies, large-scale PV and wind integration is accelerating. This study develops a comprehensive modeling approach to investigate the complex interaction among key system parameters, including the PV-wind mix, storage, curtailment, and balancing capacity, using PVGIS and Global Wind Atlas-derived data for Eritrea, addressing a gap often overlooked in most energy transition models that prioritize economic data over such interactions. The goal is to develop design and operational guidelines that address rising uncertainties in renewable-dominated grids to maximize renewable integration in future power systems. Different storage technologies are deployed to handle the daily and seasonal mismatches. The results show that diurnal storage with a 0.16 average daily demand enables 80% penetration except for a few cases. In all tested scenarios, penetration increases sharply at lower storage levels but gradually slows and stabilizes beyond a certain threshold. Beyond 80% penetration, adding diurnal storage yields minimal gains, as small increases in penetration require disproportionately large diurnal storage or excess generation. However, adding seasonal storage, with about 8 average daily demand at a RE-to-load ratio of 1.2, enables full demand coverage without additional balancing capacity. To optimize the different parameters, the system-use-index introduced in our previous work is adopted. This index provides a holistic measure of system performance by linking system efficiency with other parameters, such as storage and curtailment, thereby enhancing system flexibility and reliability. These insights contribute to the development of scalable, flexible, and sustainable future energy systems.

1. Introduction

The technical potential of Renewable Energy (RE) resources, particularly solar and wind, is vast; even a fraction of this potential is sufficient to meet global energy demand [1]. However, integrating large-scale RE systems, such as solar and wind, requires strategies to manage the inherent variability and intermittency as their increased integration brings technical challenges. Both solar and wind exhibit fluctuations across various timescales, driven by factors such as Earth's rotation, axial tilt, and atmospheric conditions. Generally, solar energy generation can vary seasonally by up to 1.5 to 6 times, depending on latitude, in addition to daily and climate-related fluctuations. Similarly, wind speed varies on both diurnal and seasonal timescales [2]. These characteristics pose technical challenges in meeting electricity demand from renewables, necessitating greater flexibility in system design and operation. It is these challenges that make energy storage essential, as it balances supply and demand [3] and provides operational reserves for large-scale integration [4]. There are various energy storage technologies, each with distinct characteristics that make them suitable for different time scales and applications. These include batteries [5],

* Correspondence to: T. T. Negash, Hungarian University of Agriculture and Life Sciences, Páter Károly u. 1, 2100, Gödöllő, Hungary.
** Correspondence to: E. Mollerstrom, Halmstad University, School of Business, Innovation and Sustainability, PO Box 823, SE-301 18, Halmstad, Sweden.
E-mail addresses: Negash.Teklebrhan.Tuemzghi@phd.uni-mate.hu, teklebrhann@gmail.com (T. Negash), erik.mollerstrom@hh.se (E. Möllerström).

https://doi.org/10.1016/j.est.2026.123040
Received 18 December 2025; Received in revised form 29 April 2026; Accepted 4 June 2026
Available online 17 June 2026

pumped hydro storage (PHS) [6], hydrogen storage [7–9], compressed air energy storage [7], and hybrid storage systems [10], such as battery-hydrogen [11,12]. The selection depends on factors such as response time, storage capacity, cost-effectiveness, and suitability for short-term or long-term energy shifting [13]. Batteries are economically competitive for diurnal applications due to their high efficiency and suitability for frequent cycling. The high round-trip efficiency, rapid response, and relatively low energy loss of Li-ion and flow batteries make them ideal for short-term energy storage [14,15]. However, batteries have short storage durations, and constructing large, underutilized systems is costly, making them less ideal for long-term energy storage. Long-term seasonal storage becomes more cost-effective at higher penetration, offering low-cost energy despite its lower efficiency and limited suitability for daily cycling [16]. Storage facilities such as PHS and hydrogen storage are better suited for long-term energy shifting. PHS is the most mature and widely used large-scale storage technology, offering high efficiency (70–85%) and long lifespans [17]. Hydrogen storage provides a flexible, scalable solution for seasonal storage with high energy density and long-term retention without significant losses [18]. Its cross-sector use in electricity and transport improves cost-effectiveness [19]. However, lower round-trip efficiency makes it better suited for seasonal than daily cycling. Hybrid storage systems, combining batteries and hydrogen, leverage short-term battery storage (4–8 h) for grid stability and hydrogen for long-term seasonal balancing (12+ hours). By enhancing reliability and increasing flexibility, this approach maximizes the sustainable and efficient use of renewable energy resources [20,21].

Extensive research has been conducted on the performance and techno-economic analysis of various storage solutions [15,19,22–26]. Denholm & Mai [27] studied the storage duration required to integrate large-scale variable renewable energy (VRE) with reduced curtailment for the Texas grid, showing that 8.5 GW of 4-h storage could lower curtailment from 11–16% to 8–10%. Solomon et al. [28–30] showed that storage sized below average daily demand can enable ~90% VRE penetration, with solar-wind complementarity further reducing storage and backup needs. High renewable shares still require multiple flexibility measures, including diurnal and seasonal storage, curtailment, and balancing capacity storage [21]. In [19], a penetration of around 90% was achieved by PV, wind, diurnal storage, and other technologies that are currently widely deployed at scale, however, the pathway to the remaining 10% remains uncertain, as these technologies aimed at full decarbonization, such as hydrogen and low-carbon fuels, have not yet been deployed at scale. Heuberger & Mac Dowell [31] studied the challenges of rapidly transitioning to 100% VRE penetration and provided insights into impacts on system operability and reliability. They argued that dispatchable balancing capacity is essential to ensure system security and supply quality for achieving 100% renewable supply. Mai et al. [32] identify a set of solutions for meeting the final 10% of demand, especially for 100% VRE targets. Some recommended pathways remain uncertain due to reliance on diverse, early-stage emerging technologies. Among the key solutions is deploying seasonal storage to address the long-term mismatch when renewable output drops for several consecutive days, such as a week. Adding more VRE or diurnal storage at high penetration levels offers a limited system benefit [33]. Diurnal storage alone is insufficient at higher penetration, as the final 10–20% requires additional system services beyond diurnal storage to achieve a fully sustainable, carbon-free grid. As discussed in Mai et al., deploying non-VRE resources like hydropower and geothermal to meet the last 10% of demand is also a feasible solution. Currently, there are no well-developed long-term (large-scale) storage options beyond hydro power, which is also limited by geographical location and water resources potential [34]. Power to Gas (P2G) technologies, such as hydrogen storage, are the most viable options. Although their technology readiness level (TRL) ranges from 3 to 7 depending on the application, mature components, such as electrolyzers and fuel cells are increasingly demonstrated at pilot and commercial scales, making it a viable option for meeting long-term seasonal fluctuations [35].

Our previous work [36], introduced a novel simulation tool to assess the interaction among system parameters, showing that diurnal storage below 0.5 average daily demand can enable 80–90% renewable penetration in Eritrea, where solar [37] and wind [38–40] resources are abundant. Building on that work [36], this study presents a methodology to evaluate the effectiveness of seasonal storage in meeting the last 20% of the demand. It provides a comprehensive system design analysis by examining key system design parameters, including the PV-wind mix, diurnal and seasonal storage requirements, curtailment strategies, and balancing capacity needs. This study investigates the technical constraints on achieving a highly renewable grid. These constraints serve as a foundational system boundary within which additional constraints, such as economic, grid operational strategy, or other factors, can be incorporated. Thus, this study aims to develop design and operational guidelines for power systems capable of managing increased uncertainties, with the ultimate goal of providing a sustainable and flexible framework to support large-scale renewable energy integration. While the findings are quantitatively referred to Eritrea and other regions with similar weather patterns, the methodology developed is robust, and it can be applied to a wider geography globally, making the approach broadly relevant for enhancing reliability, resilience, and efficiency in renewable-dominated grids.

2. Methods and data

To identify the potential wind solar sites a comprehensive literature review was conducted in addition to consulting online data bases like PVGIS and Global wind Atlas. In addition, potential solar and wind energy sites were filtered considering transmission interconnection, complementarity pattern, and proximity to load centers. Geographically distributed solar and wind sites are then selected to maximize distributed generation benefits. Distributed wind sites across the southern and northern coasts, as well as the central highlands, provide complementary patterns that effectively reduce hourly and daily fluctuations. Our analysis is based on our previously developed methodology [36], which provides detailed information on solar and wind sites. The geographical information of the selected sites is also presented in [40].

2.1. Renewable energy mix and storage simulation

A clear and transparent simulation model was developed in MATLAB environment, analyzing various sensitivities to quantify the complex interaction between key design parameters. The model operates at an hourly resolution, requiring load-demand and generation profiles. Large and diverse wind generation profiles were created by simulating the output of commercial Vestas wind turbines (V117–3.45 MW and V136–3.45 MW) using wind speed data from the PVGIS and Global Wind Atlas (GWA) databases, accounting for 13% system losses including transmission and wake losses. Turbines were selected to fit the geographical orientation of the sites and employed based on the wind speed characteristics of the selected sites. Meanwhile, solar PV generation was extracted from PVGIS for a non-tracking free-standing crystalline silicon system with optimized slope and azimuth angles. Overall, system losses of 14% (default value for PVGIS) were considered for AC generation. Further details on the solar PV and wind modeling approaches can be found in [36]. Since nationwide hourly electricity demand data is not obtained for Eritrea, we utilized Ethiopia's time series load data. Ethiopia is a neighboring country with similar climatic and cultural characteristics, and electricity consumption habits. The load data is then scaled to reflect a future scenario in which Eritrea's per capita electricity consumption reaches 2000 kWh, totaling approximately 16 TWh annually.

Generation profiles are created by varying the PV ratio from 0 to 1 in 0.1 increments, with the wind share correspondingly decreasing from 1 to 0. Though, refined the PV-wind mix mesh to smaller intervals than 0.1

steps, could improve the results, but due to computational burden we cannot perform this task at this stage of the study. Hourly net load (P_{mix}) was then calculated by subtracting load from renewable generation. This net load guided the design and dispatch of the different storage technologies utilized, assuming no transmission losses (a copper plate assumption) and focusing solely on the supply side without economic or demand-side factors.

The mismatch between generation and load is computed as:

$$P_{mix}(t) = \beta\, P_{nd}\, \alpha(r)\, \left(r\, p_{PV}(t) + (1-r)\, p_{wind}(t)\right) - P_{load}(t), \tag{1}$$

where β is a multiplier that enables oversizing the generation. Each multiplier β corresponds to a Renewable energy to load ratio (RE-to-load ratio), which is obtained by dividing the annual VRE generation by the annual load. P_{nd} the no dump capacity, $\alpha(r)$ a factor, described in detail in Appendix A, and r is the PV ratio, where $r = 0$, corresponds to wind-only scenario and $r = 1$ corresponds to solar-only scenario and $r = 0.5$, corresponds to 50–50 PV-wind scenario.

Multiple scenarios were developed to address the diurnal and seasonal mismatch between supply and demand by examining sensitivities across different storage configurations. The storage facility sizing is based on the net load (P_{mix}). Li-ion batteries are chosen for short-term diurnal storage due to their higher market maturity and energy density compared to other emerging battery technologies [41].

The diurnal storage model is formulated according to

$$S(t) = \begin{cases} S(t-\Delta t) + \min\left(\eta_{ch}\, P_{mix}(t), P_{room\_d}(t)\right)\Delta t, & \text{if } P_{mix} \geq 0 \\ S(t-\Delta t) - \min\left(-\dfrac{P_{mix}(t)}{\eta_{dis}}, -P_{room\_d}(t)\right)\Delta t, & \text{if } P_{mix} < 0 \end{cases} \tag{2}$$

where $\Delta t = 1$ h is the time step, and P_{room_d} is the hourly remaining capacity of storage during charging and discharging:

$$P_{room\_d}(t) = \begin{cases} \min\left(S_{max} - \dfrac{S(t-\Delta t)}{\Delta t}, \dfrac{S_{max}}{\Delta t_{full}}\right), & \text{if } P_{mix} \geq 0 \\ -\min\left(\dfrac{S(t-\Delta t)}{\Delta t}, \dfrac{S_{max}}{\Delta t_{full}}\right), & \text{if } P_{mix} < 0 \end{cases} \tag{3}$$

where S_{max} is the maximum capacity of the diurnal storage and Δt_{full} is the minimum time required to charge or discharge the storage fully, equivalently the energy-to-power ratio or the inverse of the maximum C-rate and Δt is time interval.

The excess power (E_p) is computed after diurnal storage is full (when $P_{mix} \geq 0$) and deficit power P_u (unmet demand) is computed after deploying, the diurnal storage (when $P_{mix} < 0$). A detailed expression is given in Appendix A.

Seasonal storage is deployed depending on penetration and curtailment limits. It is applied when penetration with diurnal storage exceeds 80% and excess generation (E_p) $\geq$ 5%, as any further increase in penetration beyond this threshold demands a substantial expansion of generation and diurnal storage capacity. Before the specified limit, no need to use seasonal storage, as diurnal storage handles the fluctuation with an efficient utilization index [16,36].

To determine charging and discharging hours, all surplus power after diurnal storage is stored in seasonal storage without any restriction. The mean hourly charging and discharging powers were then used to estimate the average storage operation duration for each.

The ability of diurnal storage to handle daily fluctuations depends on the PV-wind mix ratio and other factors. Still, longer-duration mismatches spanning multiple days to weeks necessitate the deployment of seasonal storage. Numerous studies indicate that achieving very high VRE penetration requires longer-duration storage beyond diurnal storage [16,42,43]. Though not yet widely deployed, seasonal storage solutions such as hydrogen and other fuels are recognized as key technologies that could help future grids achieve nearly 100% renewable penetration. Implementing seasonal storage enhances power system stability by reducing seasonal intermittency and significantly lowering curtailment, thereby maximizing renewable energy integration and flexibility.

Based on the performance of diurnal storage, various scenarios, conditions, and sensitivities are analyzed by combining diurnal and seasonal storage, with adjustments made to both the diurnal storage capacity and its duration to assess different system configurations. At each hour, the seasonal storage S_h is computed according to

$$S_h(t) = \begin{cases} S_h(t-\Delta t) + \min\left(\eta_{ch\_s}\, E_p(t), P_{room\_s}(t)\right)\Delta t, & \text{if } P_{mix} \geq 0 \\ S_h(t-\Delta t) - \min\left(\dfrac{P_u(t)}{\eta_{dis\_s}}, -P_{room\_s}(t)\right)\Delta t, & \text{if } P_{mix} < 0 \end{cases} \tag{4}$$

where η_{ch_s} and η_{dis_s} are the electrolyzer and fuel cell efficiencies, respectively, and P_{room_s} is the available capacity at each hour and is computed according to:

$$P_{room\_s}(t) = \begin{cases} \min\left(S_{maxh} - \dfrac{S_{h((t-\Delta t)}}{\Delta t}, \dfrac{S_{maxh}}{\Delta t_{full\_ch}}\right), & \text{if } P_{mix} \geq 0 \\ -\min\left(\dfrac{S_{h((t-\Delta t)}}{\Delta t}, \dfrac{S_{maxh}}{\Delta t_{full\_disch}}\right), & \text{if } P_{mix} < 0 \end{cases} \tag{5}$$

where S_{maxh} is the maximum capacity of the hydrogen storage, Δt_{full_ch} and Δt_{full_disch} are the charging and discharging hours for the electrolyzer and fuel cell, respectively.

Parameters, such as round-trip efficiency and battery lifetime, are taken from respective references, as given in Table 1.

When there is excess renewable generation, first, diurnal storage is charged, followed by hydrogen storage for long-term seasonal use. A similar pattern is applied during discharging diurnal, followed by seasonal storage. Excess generation is converted into hydrogen by an electrolyzer [44], which is then stored in hydrogen tanks for seasonal services through a fuel cell technology to supply electricity during times of low renewable output, effectively balancing seasonal fluctuations. If there is unmet demand, the deficit is drawn from balancing (back-up) generators, provided that battery storage and the fuel cell do not satisfy it. However, no specific storage dispatch strategy is followed to optimize storage and balancing generators; instead, it simply follows the 'use-as-available' approach, which means as long as there is energy in the storage, it is discharged at any time until demand (deficit) is satisfied.

The final curtailed energy (P_{dpf}), the charging (Ch_{lose_S}) and discharging ($Disch_{lose\_S}$) loss, the unmet demand (P_{uf}) are computed after accounting for both storage technologies (additional information in Appendix A1).

2.2. System performance indicators

The study examines the interconnected dynamics of future renewable energy systems by quantifying key indicators such as penetration, System use index (SUI), and storage utilization (SU).

Penetration (P) the share of renewables in the annual demand, is computed as

$$P = \frac{\sum P_{con}\, \Delta t}{\sum P_{load}\, \Delta t}, \tag{6}$$

where $P_{con}(t)$ is the total consumed RE that is supplied to the grid after removing the losses and the dumped part: Penetration not only refers to the renewable energy that immediately meets the load, but also the part that is met through the energy storage system (after deducting round-trip efficiency losses).

Table 1
Technical properties of storage technologies.

Storage application	Storage technology	Range of storage capacity evaluated (average daily demand)	Charging/discharging hours	Round-trip-efficiency (%)	Lifetime (calendar years)	source
Short-term (diurnal storage)	Li-ion	0.01–0.5	1/1 and 6/6	90	15	[45]
Long-term (seasonal storage)	Hydrogen	1–10	72/96	40	18	[21]

$$P_{con}(t) = P_{rew}(t) - \left(P_{dpf}(t) + Ch_{lose\_S}(t) + Disch_{lose\_S}(t)\right), \tag{7}$$

Curtailment is derived from Eq. A.6 in comparison to total renewable generation, and balancing capacity is computed from the unmet demand of Eq. A.8 (by dividing the maximum unmet demand (maximum unserved load) by the maximum load), the diurnal storage loss is small and neglected.

Storage utilization (SU) is the ratio of annual energy delivered by storage to the corresponding storage capacity.

SU can be interpreted as a number of full battery cycles per year.

$$SU = \frac{-\sum(S(t) - S(t-\Delta t))}{S_{max}}, \text{if } S(t) < S(t-\Delta t) \tag{8}$$

An ideal storage unit with 100% efficiency that is fully charged and discharged on a daily basis is expected to have a storage utilization of 365 in a normal year. To further clarify the link between the design parameters and system efficiency we have utilized the new index called system-use -index (SUI) introduced in our previous work. SUI captures the relationship and trade-offs between storage capacity and curtailment by incorporating the effect of several design parameters to reflect the full system dynamics.

System-use index (SUI) is computed as follows:

$$SUI = SU \times k \times m \times u \tag{9}$$

where the factors k, m *and* u are introduced to incorporate the key physical and design considerations that influence system design and performance in renewable-based systems. The factor k represents the contribution of storage discharge to total renewable energy consumption, indicating how effectively storage supports system demand. The factor m , defined as the ratio of average charging power to power capacity (PC), reflects the influence of storage duration (i.e., hours of storage). The factor u measures the effective utilization of renewable energy by comparing consumed renewable energy to total renewable generation; higher values indicate reduced curtailment and improved system efficiency. By accounting for all the above parameters, the index provides a comprehensive evaluation of system performance and identifies the optimal system parameters at different levels of renewable penetration.

SUI is a dimensionless quantity; it is always greater than zero ($SUI > 0$) but less than SU, ($0 < SUI < SU$), because its factors k, m and u are each less than one.

$$k = \frac{-\sum(S(t) - S(t-\Delta t))}{\sum P_{useful}}, \text{ if } S(t) < S(t-\Delta t) \tag{10}$$

$$m = \frac{\sum(S(t) - S(t-\Delta t))/N}{PC}, \text{ if } S(t) > S(t-\Delta t) \tag{11}$$

$$u = \frac{\sum P_{useful}}{\sum P_{rew}}. \tag{12}$$

where: $PC = S_{max}/_{\Delta t_{full}}$ and N is the number of observations (number of hours per year).

These indices give a comprehensive overview of system performance by examining how different interacting factors relate. SUI offers a broader assessment by connecting storage use and renewable energy generation and consumption with other factors like charging/discharging rates, and energy and power capacities.

3. Results and discussion

Our approach begins with a detailed assessment of how VRE generation varies relative to demand across various time scales. Using this time-series analysis as a foundation, we develop and propose optimized scenarios that enhance and enable large-scale renewable integration.

To verify the effectiveness and representativeness of the proxy data, we conducted a comparative statistical analysis for the two datasets. Two months of full hourly Eritrean load data for June and July of 2004 is obtained from ministry of energy and mines, Eritrea; however, the data exhibit some minor irregularities due to load shedding during specific hours in each of the analyzed months. These anomalies were corrected by applying a moving-average approximation to periods with abnormally low demand profiles. Table 2 presents a comparison of the statistical parameters between the actual and cleaned data.

As shown in the table the data provides a strong similarity, with correlation coefficients of 0.832 and 0.803 for June and July, respectively (see also Figs. B.4 and B.5 in Appendix B). Statistical indicators further confirm their close resemblance, including MAE values of 0.0737 and 0.0806, and RMSE values of 0.090 and 0.0985 for the respective months for the cleaned data sets. Although Ethiopia and Eritrea share similar climatic and cultural characteristics – and thus consumption patterns – we acknowledge the potential uncertainties in the use of Ethiopian load data as a proxy. Differences in socio-economic development, urbanization, grid reliability, and electrification trajectories may cause deviations in actual Eritrean load profiles. Though expected to have minor impact on the result and conclusion of the study, these uncertainties should be considered when interpreting the simulation results.

3.1. Mismatch pattern between VRE and demand

Understanding the mismatch between VRE generation and demand across different time scales is a fundamental requirement for designing and sizing energy storage solutions. Several studies have used net load to model storage requirements, highlighting its role in balancing grid operations [17,47,48]. In a similar approach, we begin by analyzing the mismatch between different PV-wind mix and demand. This analysis provides insights into net load variability and structural patterns under different mixing ratios. Fig. 1 illustrates how mismatch power varies with changes in the PV fraction when RE-to-load ratio of 1 is applied. The vertical axis represents the frequency, indicating the number of hours within each 100 MW mismatch interval. The frequency of positive

Table 2
Statistical comparison between actual and cleaned Eritrean load data relative to Ethiopian load data.

Data	June			July		
	Correlation coefficient	MAE	RMSE	Correlation coefficient	MAE	RMSE
Actual data	0.803	0.077	0.100	0.805	0.081	0.101
Cleaned data	0.833	0.0737	0.090	0.803	0.806	0.0985

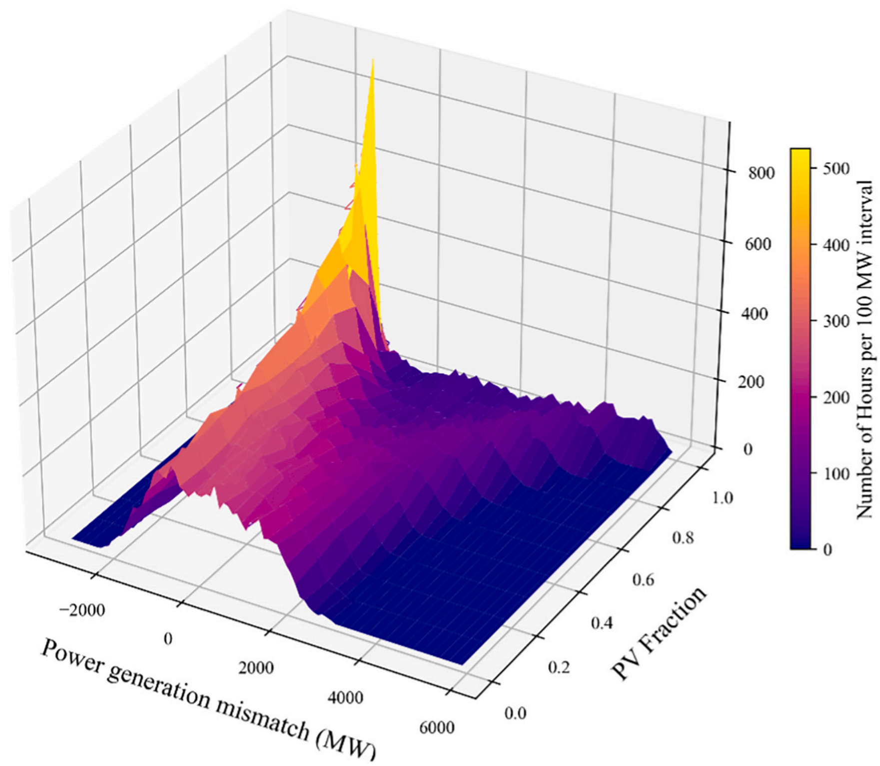

Fig. 1. Variable power generation mismatch as a function of PV fraction and number of hours per 100 MW mismatch interval (frequency).

mismatch (VRE greater than load) increases with decreasing PV fraction. However, the magnitude of the mismatch capacity decreases with the decreasing PV fraction. In contrast, both the magnitude and frequency of the negative mismatch (VRE less than load) increase with increasing PV fraction. The optimal system should have a maximum frequency at a minimum mismatch capacity (MW); however, as shown in the figure, the optimal mismatch has a lower frequency as depicted by the valley between the two peaks, particularly at solar-dominated mixes.

Fig. 1 does not give the complete picture of the netload variability in terms of time scale; therefore, understanding the time series and its time distribution in diurnal and seasonal scales is crucial for balancing supply and demand. Fig. 2 illustrates the diurnal and seasonal variability of the net load (mismatch) for the 50–50 PV-wind scenario. As shown in Fig. 2a, the mismatch is positive during the daytime, specifically from 8:00 AM to 7:00 PM, due to the diurnal cycle of solar generation. Although the RE-to-load ratio is 1, there is an hourly mismatch between generation and demand. Furthermore, there is a complete absence of solar PV at night, resulting in a negative mismatch. Solar-dominated mixes experience higher positive mismatch during the daytime and face shortages at night. In contrast, the mismatch in wind-only and wind-dominated mixes is lower and randomly distributed throughout the daytime (Fig. B.1). Such a daily mismatch can be addressed using short-term battery storage, which can store and deliver energy at high density for a few hours. Even though the daily mismatch is solved, there may be an issue of seasonal variability that remains unattended. Fig. 2b shows the characteristics of the net load in different seasons, divided into respective months. With the same RE-to-load ratio 1, over-generation occurs during the summer, as indicated by spikes in net load in June and July. Conversely, significant generation deficits are observed throughout much of the spring. In the remaining seasons, however, variability tends to fluctuate on a monthly basis rather than across entire seasons. Therefore, understanding these variabilities is

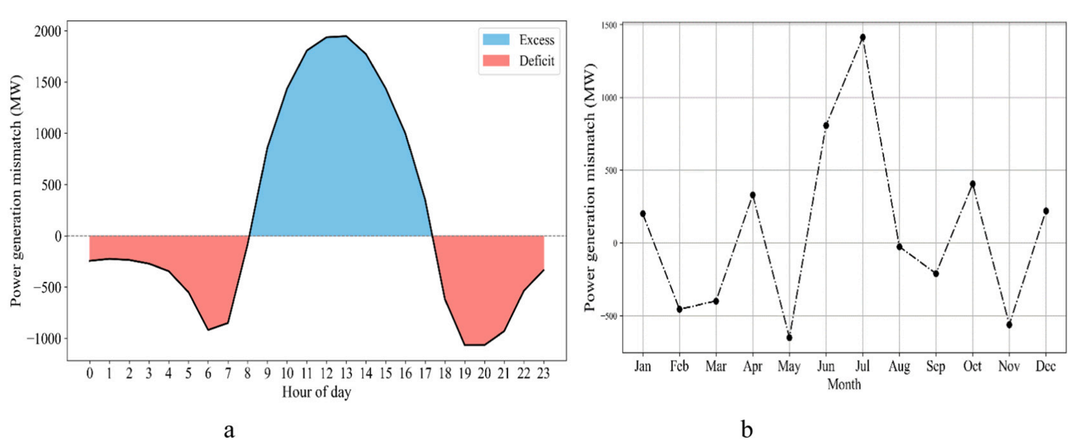

Fig. 2. Variable RE generation and demand mismatch (net-load variability) a) diurnal variability –with hourly average values b) seasonal variability- with monthly average values.

crucial for designing a system that addresses all the uncertainties of a VRE-dominated grid. Our approach utilizes various enabling tools, including diurnal storage, seasonal storage, curtailment, and balancing generators, to balance year-round hourly supply and demand. The following section will discuss the diurnal storage and its impact on achieving large-scale VRE penetration.

3.2. System performance with diurnal storage

Significant variation in penetration across different PV-wind mixes was observed when a strict no curtailment and no-storage requirement is implemented, with wind-dominated mixes achieving higher penetration levels. The best performance (in terms of load satisfied by renewables) was achieved with a PV fraction of 30%, resulting in a VRE penetration of approximately 36%. However, when the deployment of VRE resources is increased by relaxing the above requirement, a storage solution becomes necessary to utilize the resources efficiently. Based on the insights from our previous study [36], this work starts by investigating the dispatch and design aspects of diurnal storage by varying its energy capacity up to 0.8 times the average daily demand, at fixed 6 h of storage duration. Several researchers have previously demonstrated that such a storage duration can address the mismatch in timing between peak solar generation at noon and peak demand in the early evening. Moreover, diurnal storage with such a duration is cost-competitive with gas turbines for meeting peak demand [19,29,43].

The clear trend observed is that storage solutions enhance renewable penetration by reducing curtailment, especially at smaller systems depending on the PV-wind mix. Thus, we examine the effect of varying the PV-wind mix at a constant RE-to-load ratio. At a lower generation level (RE-to-load ratio 0.5), wind-dominated mix requires minimal storage to reach its maximum penetration; however, further increase in storage has a negligible effect. In contrast, solar-dominated mix requires a significantly larger storage size. At such small system sizes, wind-dominated mixes (20%–40% PV ratio) with small-sized storage of 2.5 GWh (0.06 average daily demand) have better performance in terms of storage requirement and penetration achieved. In contrast, solar-dominated mixes perform better at larger system sizes (RE-to-load ratio 1) by utilizing the storage effectively. At such a generation size, adding storage of 0.3 average daily demand shifts the optimal mix toward solar-dominated configuration, with 70%–80% PV fraction yielding 90% penetration. However, to reach 99.8% penetration, for example, in the solar-only scenario, a large amount of RE generation (RE-to-load ratio 1.87) and a substantial increase in the storage, 35 GWh (0.8 average daily demand), is required. Thus, achieving 100% RE penetration requires unreasonably large short-term storage and RE generation, which calls for complementary solutions.

In the Eritrean context, in the short term, when penetration is below 60%, wind-dominated mixes are suitable. However, as large-scale renewable deployment expands with time, solar-dominated mix combined with diurnal storage is recommended. However, further expansion to achieve 100% renewable penetration presents a new challenge due to seasonal mismatches. Simply increasing capacity in a solar-dominated mix is insufficient to meet demand, as it requires large storage to balance the diurnal and seasonal mismatch. This is specifically pronounced at higher penetration levels of above 80%. Such system characteristics, such as the requirement for impractically large installed generation capacity and/or extensive energy storage, are thoroughly discussed in Section 3.3.

The results further highlight that curtailment enhances penetration, specifically in wind-dominated mixes, due to the temporal distribution of its generation. In contrast, in solar-dominated mixes, storage is more effective than curtailment in improving penetration, as it leverages the day-night cycle of solar generation. A mix of both resources combines these advantages, enabling higher penetration while reducing curtailment and storage requirements. This study investigates the complex physical/technical interaction between such factors, as there is a fundamental challenge in designing and developing a more practical setup within a highly complex and uncertain system, as any decision may require trade-offs, potentially overlooking technical benefits that do not immediately become apparent when dealing with economic modeling.

Fig. 3 illustrates the impact of diurnal storage on penetration and storage utilization for a system with a RE-to-load ratio of 1 across three scenarios. In all cases, penetration increases sharply at lower storage sizes but gradually slows and stabilizes beyond a certain threshold, typically 7.5 GWh for wind only, 10 GWh for 50–50, and 25 GWh for solar-only scenarios. Beyond this point, additional storage yields minimal gains, as small increases in penetration requires disproportionately more diurnal storage, as shown in Fig. B.6 in the Appendix. The rate at which penetration increases with storage varies significantly across the scenarios. Similarly, adding storage initially cuts curtailment, but further capacity has little effect, as storage often stays full, causing excess generation to be curtailed and reducing overall utilization. The noticeable decrease in SU with increasing penetration, particularly at the point of inflation, strongly indicates that the diurnal storage capability to meet demand at higher penetration levels is limited to a certain threshold. Beyond which, storage becomes underutilized. This phenomenon calls for a different storage type: before the threshold diurnal storage is better suited; beyond that point the system requires long-duration seasonal storage services.

In the solar-only scenario, the diurnal cycle restricts penetration, necessitating significant storage to match supply with demand. Conversely, the wind-only case requires a small storage capacity of 7 GWh (0.16 of average daily demand) to address the temporal mismatch, due to smoother output from various sites. In the 50–50 PV-wind mix, penetration is realized through a combination of storage and curtailment. This finding is consistent with a study conducted on larger geographical scales in the U.S. [42], where reanalysis datasets (MERRA-2) with a RE-to-load ratio of 1 were applied. The penetration achieved without storage, 48% and 78% for solar and wind-only scenarios, respectively, aligns with our findings. The agreement with other studies, which used different datasets and models for other locations, presents evidence that a common physical mechanism drives the interaction between VRE generation and its matching to electricity demand.

While the rate varies across scenarios, the initial few GWh of storage capacity leads to a rapid increase in penetration, which then slows with further expansion. For instance, as shown in Fig. 3, in the 50–50 PV-wind scenario with a RE-to-load ratio of 1.0, approximately 33% of the installed 35 GWh storage capacity is effectively utilized to achieve 90% penetration. However, adding storage beyond this has minimal impact, contributing only a marginal increase in penetration. The wind-only scenario shares characteristics similar to the 50–50 PV-wind scenario. The solar-only scenario, however, exhibits a distinct pattern; it utilizes about 71% of the installed storage effectively with a storage utilization index exceeding 300 cycles per year.

The parameters discussed so far, storage, penetration, curtailment, and storage utilization, interact in complex ways and offer valuable insights into system performance. However, some parameters such as storage utilization may not reflect the whole system performance. For example, a high storage utilization index might indicate an advantage, but if the storage size is small, its actual contribution to improving system outcomes, such as boosting renewable penetration, can be minimal. They typically indicate how storage is used rather than its overall contribution to system benefits. Thus, high utilization does not always translate to greater system benefit.

The SUI shown in Fig. 4, introduced in our previous paper [36] provides an in-depth system performance assessment by connecting storage utilization and RE consumption and generation with other factors. SUI increases with storage and curtailment, reaching a peak before declining as both parameters continue to rise, clearly identifying the near-optimal system parameters that enhance overall system performance. However, SUI values should be interpreted within the context of

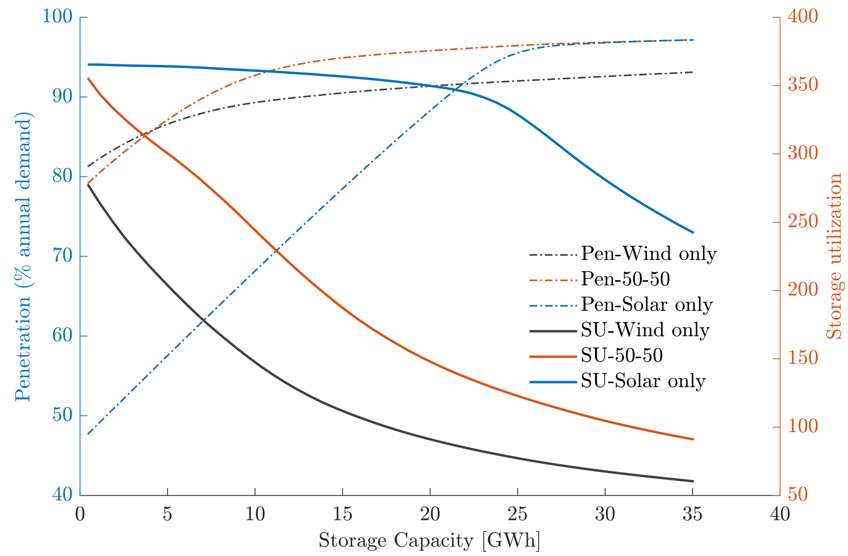

Fig. 3. Impact of storage on penetration (Pen) and storage utilization (SU) across different scenarios for a system with a RE-to-load ratio of 1.0.

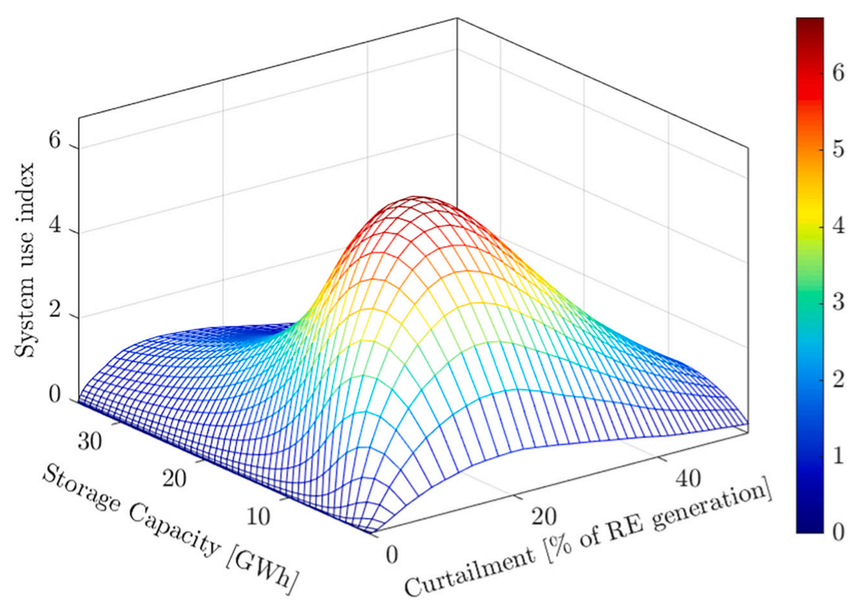

Fig. 4. System use index (SUI) for 50–50 PV-wind scenario.

each specific scenario. For instance, in the 50–50 PV-wind scenario, the plateau of the SUI ~6 indicates that the corresponding storage-curtailment combinations represent optimal or near-optimal system configurations that benefits the system most. Similarly, SUI of 1 reflects worst case scenarios, as it returns extreme curtailment–storage combinations in that specific scenario. For example, storage of 8.9 GWh (0.2 average demand) and a curtailment of 16% place on the plateau maximizes system performance. Notably, this aligns well with the observed suitable range in Fig. 3, reinforcing the validity of the SUI as a meaningful metric. While it is not inherently guaranteed that the maximum system use index corresponds to an optimal system configuration, its alignment with Fig. 3 suggests that it effectively identifies near-optimal operating conditions. This connection strengthens the argument that the SUI is a reliable indicator for balancing storage capacity and curtailment in large-scale renewable integration, depending on priorities set, whether curtailment or storage is emphasized to achieve specific penetration targets. However, the optimal parameters vary significantly across scenarios. The 50–50 PV-wind scenario achieves the highest overall performance by leveraging the advantage of complementarity and the strengths of both enabling technologies, storage, and curtailment.

3.3. RE requirement across different penetration levels

Renewable energy consumption changes significantly with increasing penetration levels. At lower penetration levels, renewables primarily displace conventional generators with minimal or without storage or grid readjustments. Fig. 5 illustrates how renewable energy requirements vary across different penetration levels for various PV-wind mixes. It highlights key characteristics of these variables beyond the no-dump capacity, the threshold beyond which the system necessitates storage, curtailment, or both. While this no-dump capacity varies depending on the PV-wind mix, the minimum penetration achievable without storage or curtailment is approximately 23.6%, a condition observed in the solar-only scenario where Fig. 5 begins. Any increase in renewable generation beyond this level requires storage/curtailment or

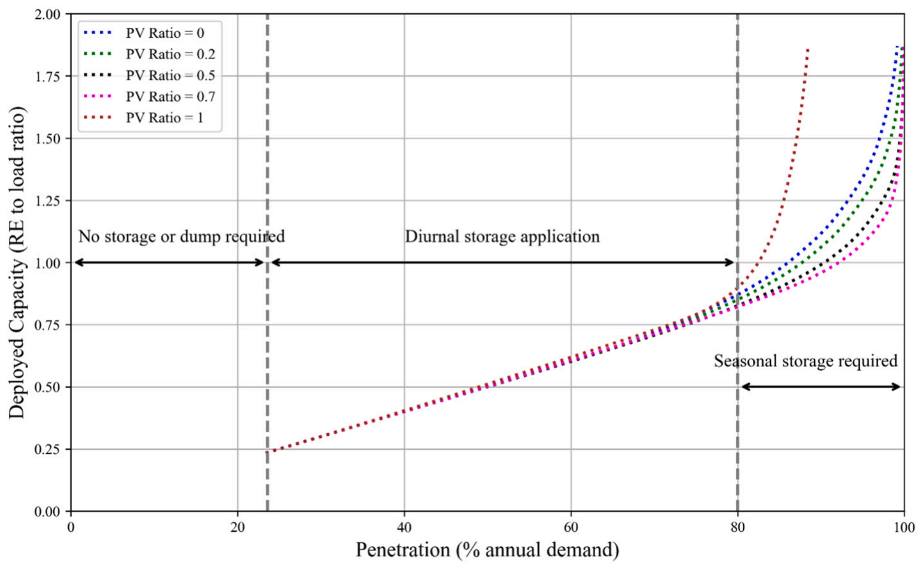

Fig. 5. Illustration of RE requirements at different stages of renewable penetration (with storage capacity 0.41 average daily demand), the steep rise in capacity addition after 80% RE penetration is due to seasonal imbalances.

both to manage fluctuations, enabling penetration up to 80%. Beyond 80% penetration, renewable deployment rises sharply, even with only a slight increase in penetration. While the RE requirement for a given penetration target varies across PV-wind mixes, this variation remains relatively minor until 80% penetration. However, beyond this point, the differences in RE requirements become more significant. Several global studies report similar findings. For example, an energy transition study examining 100% renewable energy penetration for the continental US found threshold values of 80–95% and recommend a set of solutions including seasonal storage for meeting the last ~10% [32]. A study on the Israeli grid using an advanced linear optimization model yielded comparable results, showing that diurnal storage equivalent to less than average daily demand enables up to 90% penetration [16]. Another study on the California grid investigated the impact of wind-solar complementarity on storage requirement applying different storage dispatch strategies and found that a penetration of ~85% annual demand is achievable with 20% curtailment when a diurnal storage of less than average daily demand is deployed [30]. These studies span large geographical areas and varied climates, with minor deviations resulted from grid capacity and interconnection and climatic conditions their findings are consistent regardless of methodology or geographical region covered, supporting the generalizability of our conclusion that diurnal storage effectiveness drops sharply after ~80% penetration – even across diverse climate regions.

Up to 80% RE penetration, diurnal storage plays a key role in balancing short-term fluctuations. However, beyond this threshold (80%) RE addition rises sharply due to the limitations of diurnal storage to satisfy seasonal fluctuations. Fig. 5 illustrates this challenge; RE deployment surges dramatically in this range, with a substantial increase in capacity required for even a small rise in penetration. This large generation/capacity requirement is attributed mainly to seasonal imbalances, meaning that much of the additional renewable capacity remains underutilized for most of the year and is only effective during specific seasons of peak demand or low RE generation periods, or a combination of both. This challenge becomes even more demanding when attempting to meet the demand with PV, as it requires an impractically large generation capacity and extensive storage. The marginal returns from such capacity expansion are minimal. As shown in Fig. 5, complementarity helps mitigate the steep rise in capacity additions required for higher penetration levels. However, regardless of the PV-wind mix, meeting the final 20% of the demand presents a unique challenge as it requires a substantial increase in capacity and/or significant storage deployment, as also illustrated in Fig. 3.

For a quantitative perspective, in the 50–50 PV-wind scenario, satisfying 80% of the demand requires approximately 44% of total installed RE capacity. However, meeting the last 20% of the demand requires about 56% of the total capacity. In contrast, the solar-only scenario requires around 52% of its total installed capacity to increase the penetration from 80% to its maximum of 88%. This is primarily due to the need to meet peak seasonal demand or worst-case renewable generation scenarios, where added capacity remains underutilized for extended periods. As a result, its utilization and capacity factor decrease. This situation is analogous to today's peaking plants, which supply only a small fraction of total electricity demand but account for a significant portion or share of installed capacity.

Therefore, achieving complete decarbonization and long-term energy sustainability requires not only large-scale renewable deployment but also complementary solutions such as short and long-term storage to optimize excess capacity and ensure reliable operation.

3.4. The use of seasonal storage for balancing long-term mismatch

Diurnal storage manages short-term fluctuations and facilitates a high renewable penetration of 80–90%, but its limitations become evident beyond this range. The ability of diurnal storage to handle daily fluctuations depends on the PV-wind mix ratio and other factors. Still, longer-duration mismatches spanning multiple days to weeks necessitate the deployment of seasonal storage. Numerous studies indicate that achieving very high VRE penetration requires longer-duration storage beyond diurnal storage [16,42,43]. Though not yet widely deployed, seasonal storage solutions such as hydrogen and other fuels are recognized as key technologies that could help future grids achieve nearly 100% renewable penetration. In this study seasonal storage (hydrogen) is introduced to complement the limitations of diurnal storage. Hydrogen storage is considered due to its suitability for seasonal energy shifting, high energy density, and ability to complement large-scale PV generation. Hydrogen has lower round-trip efficiency compared to most battery storage systems, however, the combination of devices used in Power-to-Gas (P2G) allows independent scaling of power and energy quantities that enable massive and long duration storage. A recent study in [21] compares the cost effectiveness of hydrogen with other long duration seasonal storage technologies such Compressed air energy storage (CAES) and pumped hydro storage (PHS) and found that hydrogen storage to be economical for long discharge duration of about

6.8 days (or more) and 16.9 days (or more) of discharge compared to CAES and PHS respectively. Moreover, a hydrogen storage with 1 week of discharge duration is found to be cost competitive if the power and energy costs are equal (or less than) ~ USD 1507 kW-1 and ~ USD 1.83 kWh-1 by 2025, respectively. This is consistent with our finding that seasonal storage equivalent to 8 days of average daily demand enables 100% penetration without balancing or back-up capacity requirement.

Despite it promising future hydrogen storage has concern regarding its management, and distribution and regulation uncertainty, in addition to relatively high costs and lower efficiencies due to the early market stage of P2G concepts. Moreover, most hydrogen-related components are still at relatively early stages of development, with technology readiness levels (TRLs) generally falling between 3 and 7, depending on the specific application. However, certain key technologies – such as electrolysers and fuel cells – have advanced significantly and are now being deployed and validated at pilot and even commercial scales. This growing maturity and real-world demonstration strengthen the case for using hydrogen as a credible option in long-term energy storage models [35].

Implementing seasonal storage enhances power system stability by reducing seasonal intermittency and significantly lowering curtailment, thereby maximizing renewable energy integration and flexibility.

Various conditions are examined for different configurations by adjusting the energy and power capacity of the diurnal storage to assess the impact of seasonal storage. Near-optimal parameters obtained from Figs. 3 and 4 are the upper limits for diurnal storage, after which seasonal storage is introduced. Fig. 6 illustrates the penetration levels achieved when seasonal storage, along with diurnal storage with a 6-h duration, is applied across the three scenarios analyzed. Diurnal storage is used for lower penetration levels (< 80%). In comparison, seasonal storage is utilized at higher penetration levels, reaching approximately 100% and 98% at 180 GWh (equivalent to 4 average daily demand) for the 50–50 PV-wind and wind-only scenarios, respectively. In contrast, the solar-only scenario requires a larger storage capacity to achieve the same penetration level. In this scenario, increasing diurnal storage from 0.16 to 0.5 average daily demand (Fig. 6b) enables 100% penetration at significantly reduced seasonal storage, unlike Fig. 6a, where 100% penetration is not achieved even at the maximum seasonal storage size. This is because diurnal storage is efficiently utilized across wide range of storage capacities in solar-only scenario (as demonstrated in Fig. 3). This shows that storage is advantageous in a solar-only scenario at all levels of renewable penetration. Regardless of the PV-wind mix, seasonal storage plays a crucial role in enabling higher renewable penetration by mitigating seasonal mismatches.

Since seasonal storage is mainly used during periods of low generation, peak demand, or both, its utilization is expected to be limited to a few days each year. As shown in Fig. 7, even in the most suitable range, SU varies from about 20 to 30 days per year, and the maximum value occurs for storage sizes ranging from a few GWh to 100 GWh. Analyzing the storage utilization index offers valuable insights into how effectively the allocated storage is used, ensuring it is not underutilized.

Fig. 7 presents how the storage is utilized in the 50–50 scenario, demonstrating various combinations of storage and curtailment that maximize its utilization. For instance, achieving 100% renewable penetration requires 180 GWh (equivalent to 4 average daily demand) of hydrogen storage, with storage utilization of 20 full days with minimal curtailment of approximately 7%. However, as storage capacity decreases, utilization improves. While storage utilization provides critical insights into how deployed storage is utilized, it does not capture the complete system dynamics, as it is limited to storage parameters without integrating broader system variables. To address this limitation, the SUI discussed in Section 3.2 and illustrated in Fig. 8 offers a more comprehensive measure by integrating all key design parameters, such as annual discharge, total storage capacity, and net renewable energy consumption, into a single metric that captures system dynamics and performance within the context of broader energy infrastructure considerations.

As shown in Fig. 8, SUI initially increases with storage and curtailment but declines beyond a certain threshold. The optimal combination lies within the plateau, where various storage and curtailment pairs contribute to an efficient balance. For example, in the 50–50 PV-wind scenario, a storage capacity of 100 GWh (about 2.3 average daily demand), combined with a curtailment level of 10%, falls within this plateau and enables a renewable penetration of approximately 95%. In the wind-only scenario, a similar storage capacity with slightly higher curtailment achieves around 94% penetration. This is far below the maximum storage requirements reported in several studies reviewed in [34], where achieving 95% renewable penetration required storage capacities of less than 1.5% of annual demand. The results indicate that the optimal SUI varies slightly between scenarios: the wind-only scenario benefits more from curtailment, whereas the 50–50 PV-wind scenario favors increased storage, as the 50% solar PV share benefits more from energy retention.

SUI behaves differently in the solar-only scenario (Fig. B.4, Appendix B). Unlike the wind-only and 50–50 scenarios, the index in the solar-only

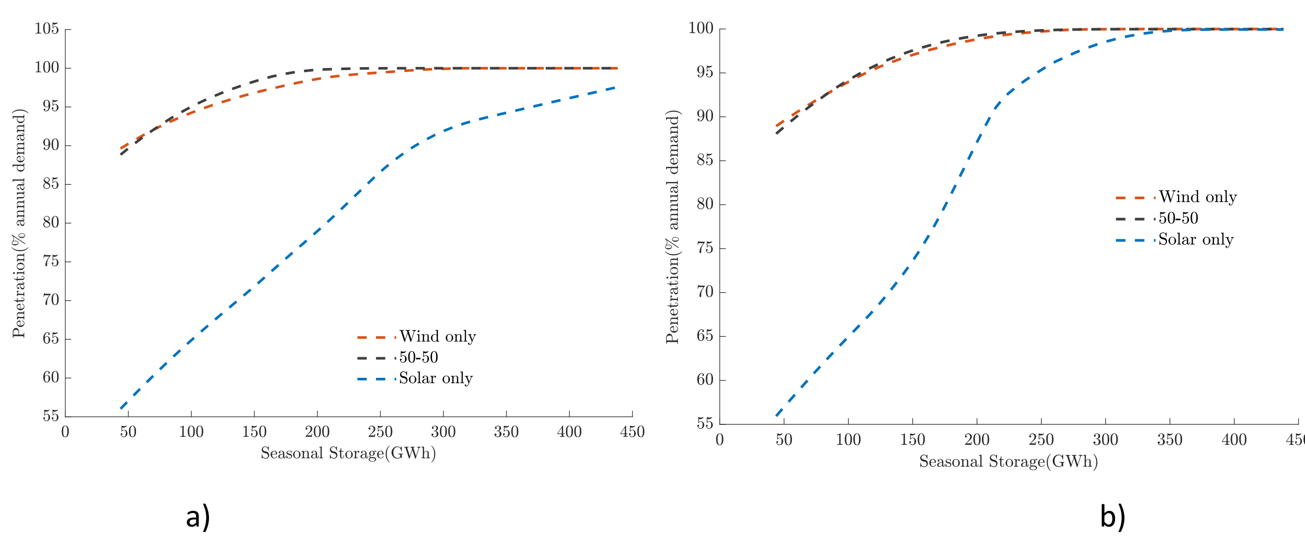

Fig. 6. Achieving high RE penetration using seasonal storage combined with diurnal storage when diurnal storage capacities of (a) 0.16 and (b) 0.5 times the average daily demand are added, at a RE-to-load ratio of 1.3.

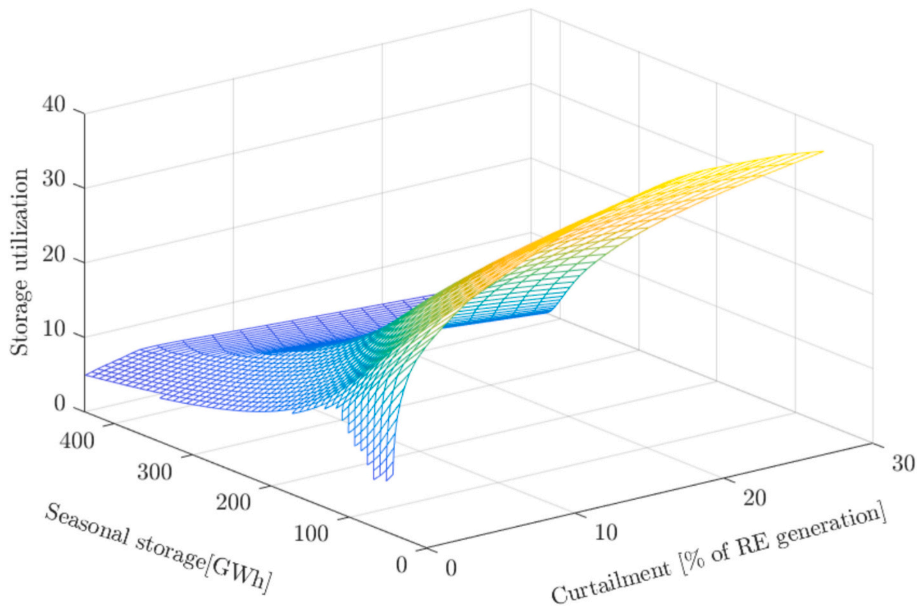

Fig. 7. Seasonal storage utilization for 50–50 scenario, with diurnal storage of 0.16 average daily demand with 6 h duration.

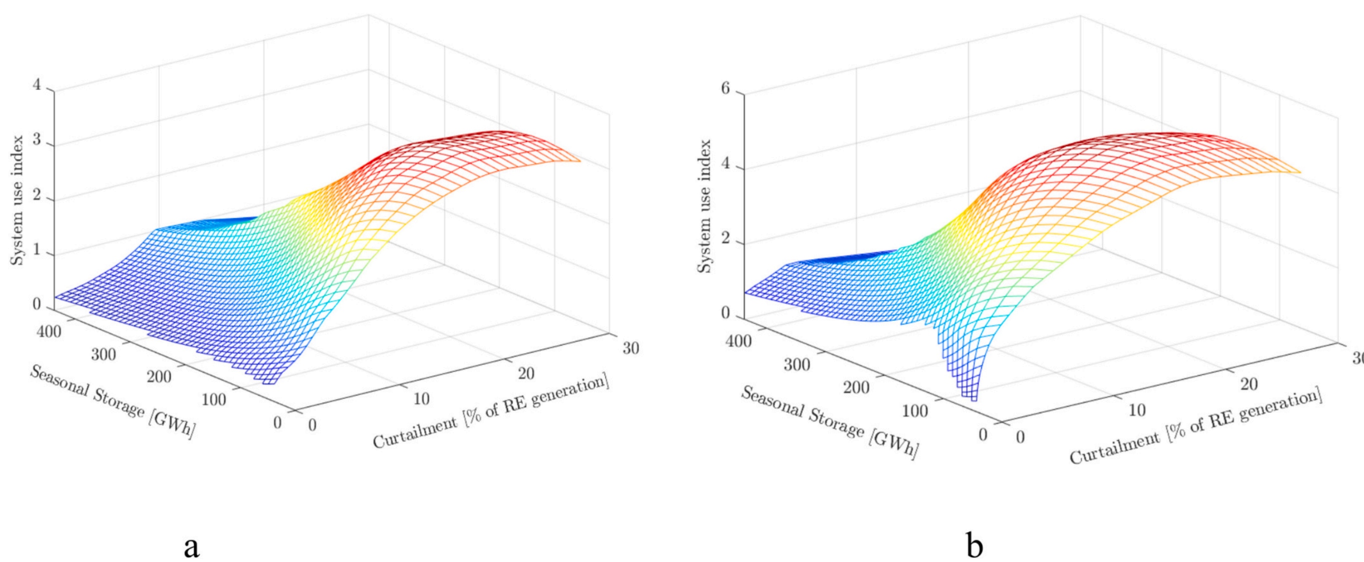

Fig. 8. System use index a) wind only b) 50–50 PV-wind scenario.

case continues to increase with both storage and curtailment. The near-optimal balance is reached at approximately 200 GWh of storage with 15% curtailment. Regardless of the generation mix, increasing seasonal storage beyond 250 GWh (equivalent to 5.7 average daily demand) yields minimal additional benefits. For comparison, the results of five German and European studies were synthesized in [49] and they found that optimal storage capacities were found between 12 and 32 days of average load. However, such a large-scale deployment of hydrogen brings some uncertainties, such as the high initial cost of producing and storing hydrogen, which requires a large investment. To make hydrogen storage a financially viable option, the overall cost of electrolyzers and fuel cells should be significantly reduced [50]. According to forecasts, hydrogen has a bright future and costs are expected to reduce with mass production, and it will play a crucial role in energy to complete decarbonization 100% renewable power [51] Moreover, a study conducted considering fully renewable grids shows that for long-term seasonal services, hydrogen storage is economically and technologically feasible compared to other (diurnal) storage options such as Li-ion batteries and vanadium redox-flow systems [52].

The impact of diurnal storage on seasonal storage requirements is then examined by changing the hours of diurnal storage to 1 h. Short storage hours are well-suited for short-term, high-intensity power delivery with short but high renewable generation peaks. With a 1-h duration, penetration slightly improves but demands more seasonal storage and balancing capacity. The near-optimal system parameters identified using the SUI and the maximum penetration achieved are presented in Table B1.

In the solar-only scenario, diurnal storage of 0.16 average daily demand with 1-h duration reaches 63% penetration with significant curtailment (at around RE-to load ratio 1). This configuration requires a slightly larger seasonal storage capacity of approximately 10 average daily demand to raise the penetration to 98%. In contrast, for the same diurnal storage, the 50–50 scenario achieves 80% penetration with lower curtailment, and seasonal storage of about 5 average daily demand is needed to reach this penetration (98%). A moderate increase in diurnal storage to 0.5 average daily demand with a 6-h duration requires lower seasonal storage to reach near-optimal points. A trade-off relationship exists between increasing the diurnal storage and the seasonal storage requirement. These findings are well aligned with [53] where more efficient (80%) storage with a few hours (4 h) capacity was found more suitable to achieve lower than 82% penetration, whereas less efficient storage (30%) with longer duration hours (168 h) was better for higher penetration levels.

The preceding discussion showed that various combinations of storage and curtailment, positioned within the plateau of each figure, provide the most significant benefits to the system. These parameters, in turn, function as foundational boundaries for advanced models that incorporate additional constraints, such as electrical and economic parameters, which can be fine-tuned to enhance overall system performance.

3.5. Dispatchable balancing (back-up) requirements

The results so far show that VRE can meet annual demand with near-100% reliability when supported by various forms of storage and curtailment. However, even at high penetration levels, there are still periods, particularly on an hourly scale, where significant unmet demand persists. To maintain grid stability and reliability, bridging these gaps requires dispatchable renewables like hydropower, geothermal, or biomass, and fast-response plants. Relying only on diurnal storage demands large-scale dispatchable balancing capacity for extreme conditions. Adding seasonal storage helps reduce balancing needs by covering seasonal peaks and low-generation periods.

Fig. 9 shows the balancing capacity required under varying storage and curtailment levels for the 50–50 PV-wind scenario. Optimizing both parameters improve system performance by boosting renewable penetration and reducing balancing needs. At all storage levels, curtailment lowers balancing capacity. For example, with seasonal storage equal to 5 average daily demand and a RE-to-load ratio of 1, a balancing capacity of 82% is required with negligible curtailment. Raising the RE-to-load ratio to 1.2 lowers the balancing capacity to 74%. Increasing the generation to 1.4, balancing capacity drops to 28%, achieving 99.7% penetration.

At a RE-to-load ratio of 1.2, a complete decarbonization (100% of renewable energy) is feasible without requiring any balancing capacity (it means there is no unserved load in each hour of the year) when seasonal storage of about 8 average daily demands is deployed. At this generation and storage level, no balancing is required for mixes of 0.3 to 0.8 PV ratio. However, outside this range, significant balancing capacity is necessary, especially in wind-only and solar-only scenarios, even with generation and storage are at their maximum values of 1.4 and 10, respectively.

In all evaluated scenarios, except the wind-only case with zero solar share, nighttime hours present the biggest challenge for meeting demand, even with seasonal storage. In the wind-only scenario, some hours also see significant unmet demand due to the high variability of wind generation, causing mismatches with peak demand in certain seasons.

Our storage dispatch strategy is based on a use-as-available approach; however, effective storage dispatch and management strategies can reduce balancing capacity significantly without affecting total renewable penetration. If storage is depleted too quickly to meet immediate demand, it may be unavailable when needed later, increasing dependence on balancing capacity. A more controlled and gradual discharge strategy, distributing stored energy more evenly over time, can mitigate this issue by spreading unmet demand more evenly rather than concentrating it during peak periods. This approach also yields economic benefits by reducing the need for unnecessarily large-scale back-up capacity deployment, which is often subtly utilized for a few critical days in a year when demand peaks or weather conditions are extreme. Furthermore, power operators can optimize system performance by strategically dispatching storage and generation, provided that accurate demand and generation forecasts are available in advance.

4. Conclusion

This study uses a simulation-based approach to optimize renewable energy integration, employing one year of historical weather data from Eritrea. It systematically analyzed different scenarios by examining storage configurations and sensitivities to identify the best strategies for

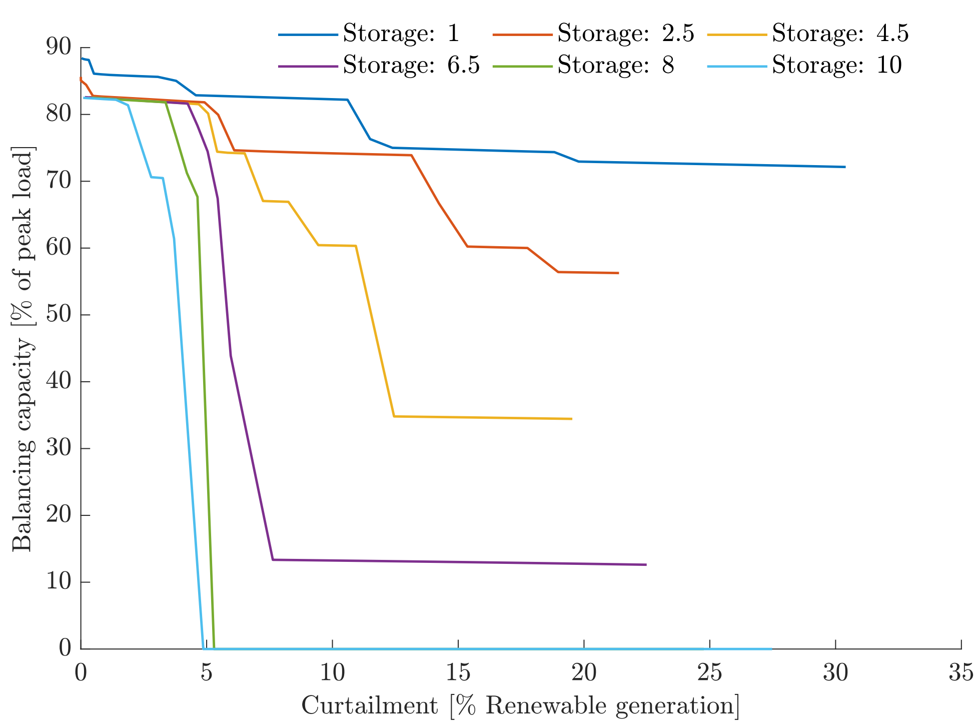

Fig. 9. Impact of storage and curtailment combinations on reducing balancing requirements in 50–50 PV-wind scenario (Storage unit: average daily demand).

increasing renewable energy use. The findings highlight that storage and curtailment are crucial for boosting renewable energy integration, with diurnal and seasonal storage addressing both short- and long-term fluctuations. Diurnal storage effectively manages short-term variability and boosts penetration, but its benefits diminish beyond a certain point. The SUI is used to optimize system parameters, offering a unified metric to assess performance and identify near-optimal system configurations. The analysis shows that diurnal storage of about 0.16 times the average daily demand (except solar-only) supports up to 80% penetration at an RE-to-load ratio of 1. Curtailment also improves integration but has diminishing returns beyond a certain level.

A similar trend is observed with renewable deployment: penetration increases steadily until 80%, but achieving full decarbonization (100%) requires a disproportionately large capacity expansion (excess generation). For example, in the 50–50 PV-wind scenario, the final 20% of demand requires about 56% of the total installed storage capacity. This challenge is even worse in a solar-only scenario, where extensive generation and storage are needed. The results indicate that the large storage and generation requirements come from seasonal variability in solar and wind, as well as peak seasonal demand. Long-term variability limits the effectiveness of diurnal storage. Adding seasonal storage, about 8 times the average daily demand with a RE-to-load ratio of 1.2, enables complete decarbonization without balancing capacity needs. The most challenging hours, requiring about 82% balancing capacity, occur when solar is unavailable at night. However, optimizing storage dispatch and implementing effective management strategies can significantly reduce excessive balancing capacity needs without compromising total renewable penetration. Additionally, solutions like flexible demand management, hours-ahead generation forecasting, and grid interconnections can further enhance system optimization. The study further employs a technical-first approach to system design, emphasizing the interplay of resource mix, storage, curtailment, and balancing requirements. Unlike economic optimization models that pay little attention to the complex interaction among these parameters, our study clearly assesses their impact on system performance.

It should be noted that this kind of study relies on several simplifying assumptions – including copperplate transmission, a use-as-available storage dispatch strategy, and a technology-first approach – to model future energy trends while reducing modeling complexity and computational burden. We acknowledge that these simplifications may over - or underestimate simulation results, thus our findings provide only a general overview of trends in renewable-dominated grids. Despite these limitations, the methodological approach introduced in this study effectively identifies multiple options for significantly improving the performance of future grids. The findings provide a structured framework for identifying system parameters that enhance efficiency and system reliability. This study lays a strong foundation for developing advanced models, incorporating economic, grid-related, and policy constraints for comprehensive RE integration. The analytical framework and methods proposed in this paper are broadly applicable, although the quantitative results are specific to regions with climate and resource characteristics similar to Eritrea (e.g., high solar irradiance and particular wind patterns); nevertheless, the methodology itself is robust and can be adapted to other geographical and system contexts.

CRediT authorship contribution statement

Teklebrhan Negash: Writing – review & editing, Writing – original draft, Visualization, Validation, Software, Methodology, Investigation, Formal analysis, Data curation, Conceptualization. **Solomon A.A.:** Writing – review & editing, Visualization, Validation, Supervision, Software, Methodology, Investigation, Formal analysis, Data curation, Conceptualization. **Fredric Ottermo:** Writing – review & editing, Visualization, Validation, Supervision, Software, Methodology, Investigation, Formal analysis, Data curation. **Erik Möllerström:** Writing – review & editing, Visualization, Validation, Supervision, Investigation, Formal analysis, Data curation. **Seres István:** Writing – review & editing, Visualization, Validation, Supervision, Resources. **Farkas István:** Writing – review & editing, Visualization, Validation, Supervision, Resources.

Funding

This work was supported by the Stipendium Hungaricum Programme and by the Mechanical Engineering Doctoral School, Hungarian University of Agriculture and Life Sciences, Gödöllő, Hungary.

Declaration of competing interest

The authors declare that they have no known competing financial interests or personal relationships that could have appeared to influence the work reported in this paper.

Appendix A

A.1. Renewable generation mix and storage modeling

The various mixes of PV-wind are computed by

$$P_{\mathrm{rew}}(t) = P_{\mathrm{nd}}\,\alpha(r)\,\left(r\,p_{\mathrm{PV}}(t) + (1-r)\,p_{\mathrm{wind}}(t)\,\right), \tag{A.1}$$

where $p_{\mathrm{PV}}(t)$ and $p_{\mathrm{wind}}(t)$ are the PV and wind generation at hour t relative to their peak capacities, respectively, and r is solar PV ratio, P_{nd} is the minimum no-dump capacity, and $\alpha(r)$ is a factor. Where $r = 0$ corresponds to 100% wind (wind only scenario) and $r = 1$ corresponds to 100% solar (solar only scenario) and $r = 0.5$ corresponds to 50% PV and 50% wind (50–50 PV-wind scenario).

$\alpha(r)$ is determined from the expression:

$$\sum_t \alpha(r)(r\,p_{\mathrm{PV}}(t) + (1-r)\,p_{\mathrm{wind}}(t)\,) = \mathrm{const}, \tag{A.2}$$

The no-dump capacity (P_{nd}) is computed as:

$$P_{nd} = \frac{P_{\mathrm{load}}(t)}{(r\,p_{\mathrm{PV}}(t) + (1-r)\,p_{\mathrm{wind}}(t)\,)}\ , \tag{A.3}$$

The excess power (E_{p}) after diurnal storage (when $P_{\mathrm{mix}} \geq 0$)

$$E_p(t) = P_{\mathrm{mix}}(t) - \min\left(P_{\mathrm{mix}}(t)\ ,\ \ \frac{P_{\mathrm{room\_d}}(t)}{\eta_{\mathrm{ch}}}\right), \tag{A.4}$$

The deficit power P_u (unmet demand) after deploying diurnal storage is (when $P_{mix} < 0$)

$$P_u(t) = -P_{mix}(t) - \min(-P_{mix}(t), -\eta_{dis} P_{room\_d}(t)), \tag{A.5}$$

The final curtailed energy (P_{dpf}) at time t after accounting for both storage technologies is:

$$P_{dpf}(t) = E_p(t) - \min\left(E_p(t), \frac{P_{room\_s}(t)}{\eta_{ch\_s}}\right), \quad \text{if } P_{mix} \geq 0 \tag{A.6}$$

Similarly, the charging (Ch_{lose_S}) and discharging ($Disch_{lose\_S}$) loss is computed from eqns. A.5 and A.6, respectively

$$Ch_{lose\_S}(t) = (1 - \eta_{ch\_s}) \min\left(E_p(t), \frac{P_{room\_s}(t)}{\eta_{ch\_s}}\right), \tag{A.7}$$

The unmet demand (P_{uf})

$$P_{uf}(t) = P_u(t) - \min(P_u(t), -\eta_{dis\_s} P_{room\_s}(t)), \quad \text{if } P_{mix} < 0 \tag{A.8}$$

$$Disch_{lose\_S}(t) = \left(\frac{1}{\eta_{dis\_s}} - 1\right)\left(\min\left(\frac{P_u(t)}{\eta_{dis\_s}}, P_{room\_s}(t)\right)\right) \tag{A.9}$$

Appendix B

B.1. Power generation mismatch with load demand

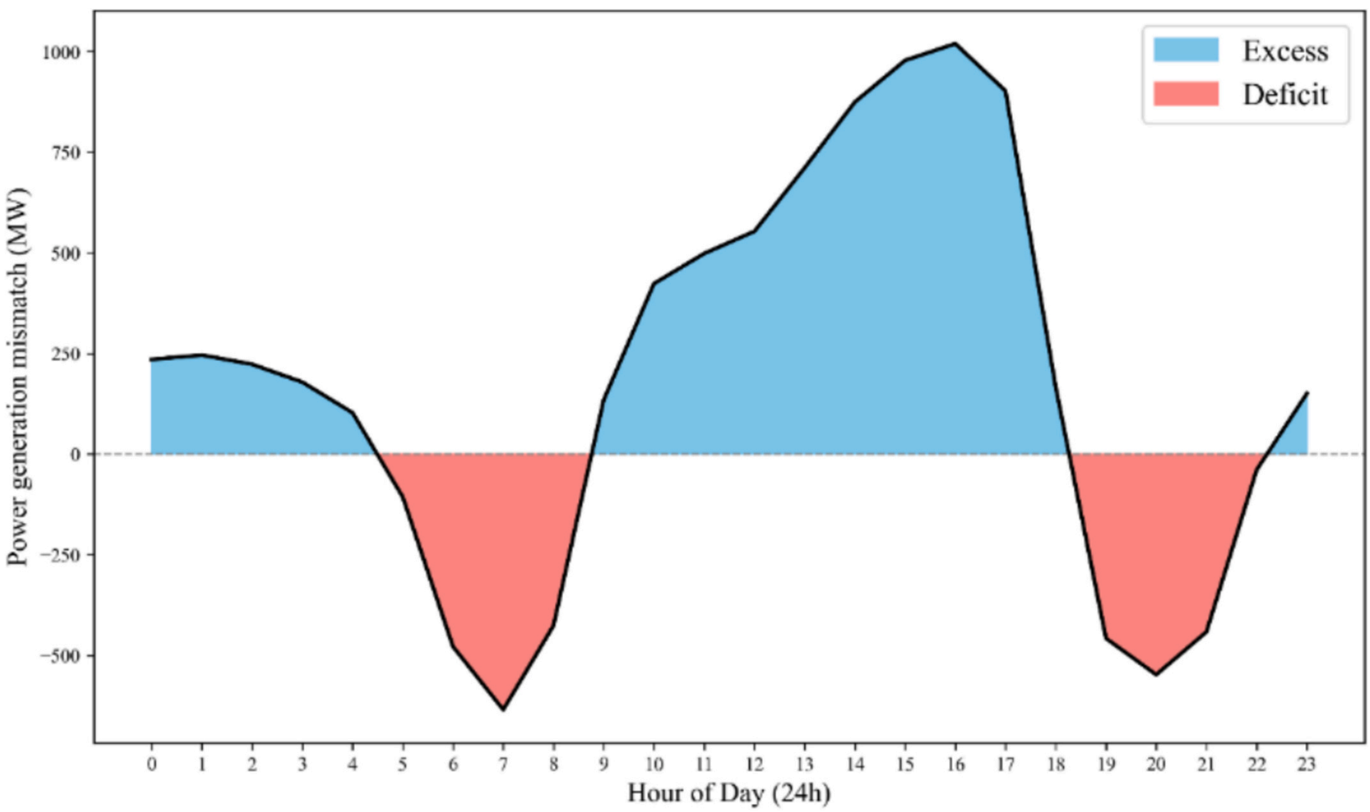

Fig. B.1. RE generation- demand mismatch wind only scenario (RE-to-load ratio 1).

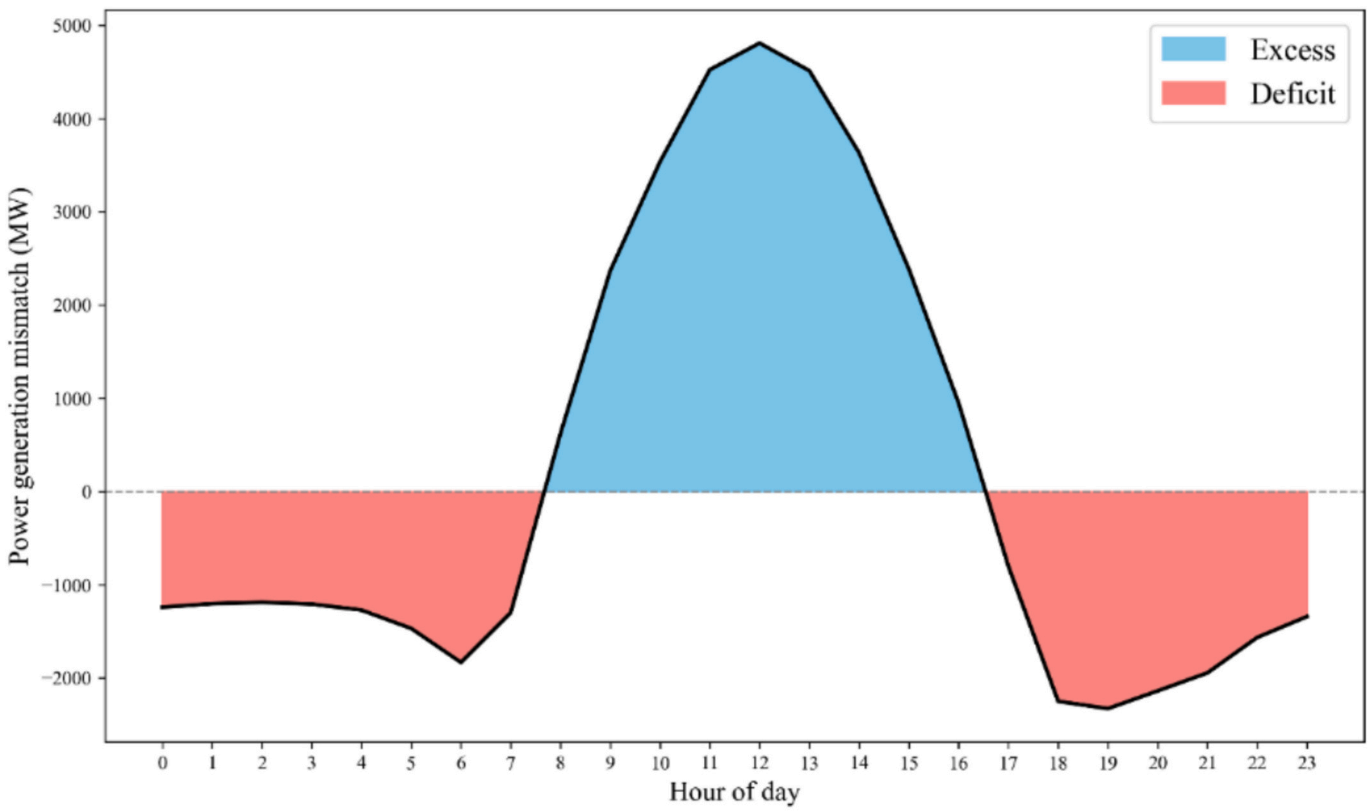

Fig. B.2. RE generation-demand mismatch solar only scenario (RE-to-load ratio 1).

B.2. The use of seasonal storage for balancing long-term mismatch

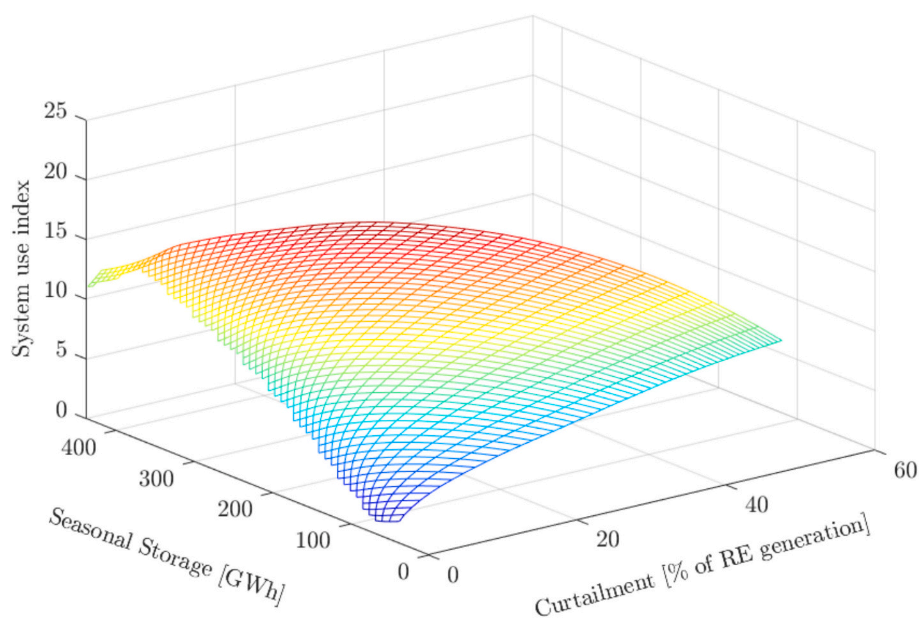

Fig. B.3. System use index for solar-only scenario.

Table B.1
Near-optimum system parameters, penetration (Pen), curtailment (Cur), and seasonal storage (S.S) with diurnal storage for 1 and 6 h duration and 0.16 average daily demand.

Scenario	Diurnal storage 1 h duration				Diurnal storage 6 h duration			
	Pen (%)	Cur (%)	S.S (av. Daily demand)	Max. Pen (%)	Pen (%)	Cur (%)	S.S. (av. Daily demand	Max. Pen
Solar only	83	13.6	4.9	99	80	14.5	4.7	99
50–50	93	11.3	2.3	100	92.5	13	2.2	100
Wind only	92.2	17	2.1	100	91	18	1.9	100

B.3. Load data validation

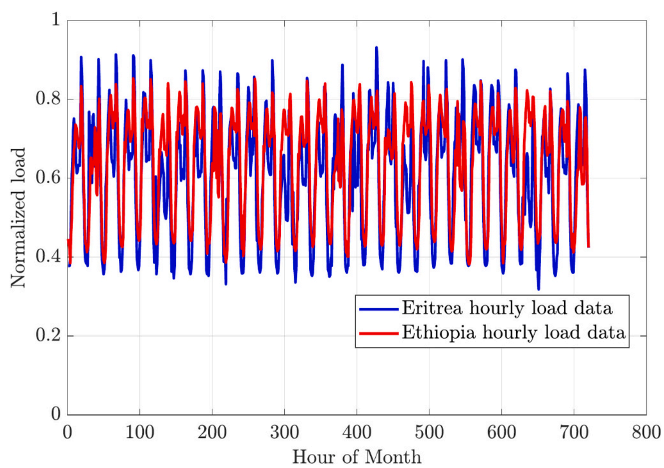

Fig. B.4. Hourly load data comparison for Eritrea (cleared data) and Ethiopia (June, 2004).

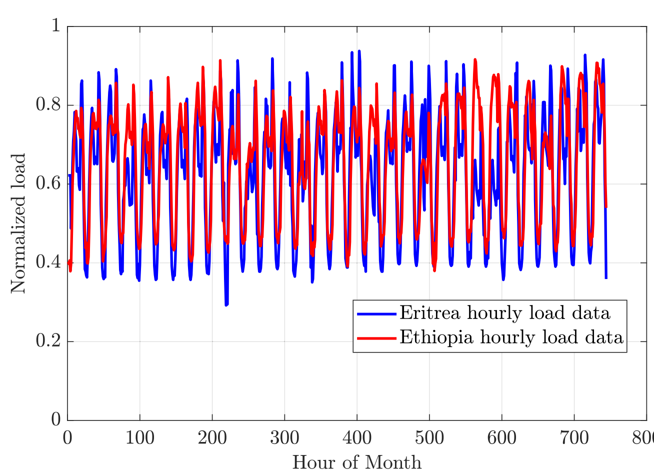

Fig. B.5. Hourly load data comparison for Eritrea (cleaned data) and Ethiopia (July, 2004).

B.4. Diurnal storage vs penetration

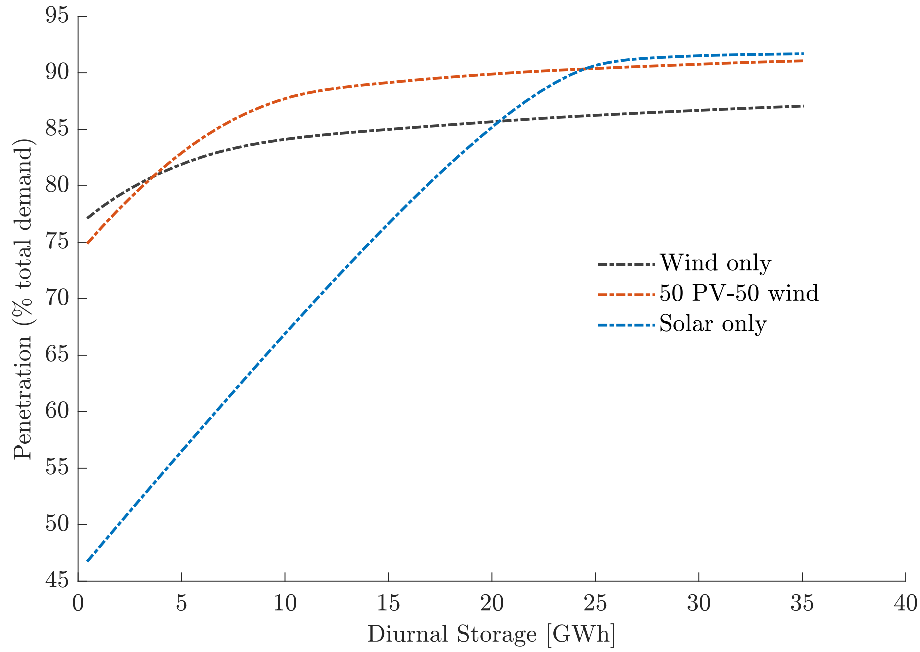

Fig. B.6. Penetration versus diurnal storage for the three scenarios.

Data availability

Data will be made available on request.

References

[1] B. François, M. Borga, J.D. Creutin, et al., Complementarity between solar and hydro power: sensitivity study to climate characteristics in Northern-Italy, Renew. Energy 86 (2016) 543–553.
[2] F.M. Mulder, Implications of diurnal and seasonal variations in renewable energy generation for large scale energy storage, J. Renew. Sustain. Energy 6 (2014), https://doi.org/10.1063/1.4874845. Epub ahead of print.
[3] S. Saha, G. Saini, S. Mishra, et al., A comprehensive review of techno-socio-enviro-economic parameters, storage technologies, sizing methods and control management for integrated renewable energy system, Sustain. Energy Techn. and Assess. 54 (2022) 102849.
[4] B. Zakeri, S. Syri, Electrical energy storage systems: a comparative life cycle cost analysis, Renew. Sust. Energ. Rev. 42 (2015) 569–596.
[5] M.S. Javed, A. Song, T. Ma, Techno-economic assessment of a stand-alone hybrid solar-wind-battery system for a remote island using genetic algorithm, Energy 176 (2019) 704–717.
[6] M. Guezgouz, J. Jurasz, B. Bekkouche, et al., Optimal hybrid pumped hydro-battery storage scheme for off-grid renewable energy systems, Energy Convers. Manag. 199 (2019) 112046.
[7] J.P. Torreglosa, P. García, L.M. Fernández, et al., Energy dispatching based on predictive controller of an off-grid wind turbine/photovoltaic/hydrogen/battery hybrid system, Renew. Energy 74 (2015) 326–336.
[8] P. Gabrielli, A. Poluzzi, G.J. Kramer, et al., Seasonal energy storage for zero-emissions multi-energy systems via underground hydrogen storage, Renew. Sust. Energ. Rev. 121 (2020) 109629.
[9] R. Zhang, X. Zhao, Y. Liu, et al., Development pathway and influencing factors of hydrogen energy storage accommodating renewable energy growth, J. Energy Storage 87 (2024) 111441.
[10] Y. Shao, Y. Lin, C. Yang, et al., Enhancing the integration of PV and coal-fired power plant for low-carbon, low-cost, and reliable power supply through various energy storage systems, Sustain. Energy Technol. Assess. 69 (2024) 103924.
[11] Z. Li, Y. Liu, M. Du, et al., Modeling and multi-objective optimization of a stand-alone photovoltaic-wind turbine-hydrogen-battery hybrid energy system based on hysteresis band, Int. J. Hydrog. Energy 48 (2023) 7959–7974.
[12] X. Chen, Y. Wang, Z. Wu, et al., Capacity expansion model for multi-temporal energy storage in renewable energy base considering various transmission utilization rates, J. Energy Storage 98 (2024) 113145.
[13] A.A. Kebede, T. Kalogiannis, J. Van Mierlo, et al., A comprehensive review of stationary energy storage devices for large scale renewable energy sources grid integration, Renew. Sust. Energ. Rev. 159 (2022) 112213.
[14] P. Lu, P. Leung, H. Su, et al., Materials, performance, and system design for integrated solar flow batteries – a mini review, Appl. Energy 282 (2021) 116210.
[15] T. Liu, J. Li, Z. Yang, et al., Evaluation of the short- and long-duration energy storage requirements in solar-wind hybrid systems, Energy Convers. Manag. 314 (2024) 118635.
[16] A.A. Solomon, D. Bogdanov, C. Breyer, Curtailment-storage-penetration nexus in the energy transition, Appl. Energy 235 (2019) 1351–1368.
[17] J. Dujardin, A. Kahl, B. Kruyt, et al., Interplay between photovoltaic, wind energy and storage hydropower in a fully renewable Switzerland, Energy 135 (2017) 513–525.
[18] H. Breunig, F. Rosner, S. Saqline, et al., Achieving gigawatt-scale green hydrogen production and seasonal storage at industrial locations across the U.S, Nat. Commun. 15 (2024) 9049.
[19] P. Denholm, P. Brown, W. Cole, et al., Examining supply-side options to achieve 100% clean electricity by 2035, Nrel (2022) 161.
[20] Y. Qiu, Q. Li, Y. Ai, et al., Optimal scheduling for microgrids considering long-term and short-term energy storage, J. Energy Storage 93 (2024), https://doi.org/10.1016/j.est.2024.112137. Epub ahead of print.
[21] O.J. Guerra, J. Zhang, J. Eichman, et al., The value of seasonal energy storage technologies for the integration of wind and solar power, Energy Environ. Sci. 13 (2020) 1909–1922.
[22] E. Rey-Costa, B. Elliston, D. Green, et al., Firming 100% renewable power: costs and opportunities in Australia's National Electricity Market, Renew. Energy 219 (2023) 119416.
[23] J. Graça Gomes, J. Jiang, C.T. Chong, et al., Hybrid solar PV-wind-battery system bidding optimisation: a case study for the Iberian and Italian liberalised electricity markets, Energy 263 (2023), https://doi.org/10.1016/j.energy.2022.126043. Epub ahead of print.
[24] M. Child, C. Breyer, The role of energy storage solutions in a 100% renewable Finnish energy system, Energy Procedia 99 (2016) 25–34.
[25] W. Cole, A.W. Frazier, Cost Projections for Utility-Scale Battery Storage: 2023 Update, National Renewable Energy Laboratory, 2023, p. 20.
[26] F. Cebulla, J. Haas, J. Eichman, et al., How much electrical energy storage do we need? A synthesis for the U.S., Europe, and Germany, J. Clean. Prod. 181 (2018) 449–459.
[27] P. Denholm, T. Mai, Timescales of energy storage needed for reducing renewable energy curtailment, Renew. Energy 130 (2019) 388–399.
[28] A.A. Solomon, M. Child, U. Caldera, et al., How much energy storage is needed to incorporate very large intermittent renewables? Energy Procedia 135 (2017) 283–293.
[29] A.A. Solomon, D. Faiman, G. Meron, Properties and uses of storage for enhancing the grid penetration of very large photovoltaic systems, Energy Policy 38 (2010) 5208–5222.

[30] A.A. Solomon, D.M. Kammen, D. Callaway, Investigating the impact of wind-solar complementarities on energy storage requirement and the corresponding supply reliability criteria, Appl. Energy 168 (2016) 130–145.

[31] C.F. Heuberger, N. Mac Dowell, Real-world challenges with a rapid transition to 100% renewable power systems, Joule 2 (2018) 367–370.

[32] T. Mai, P. Denholm, P. Brown, et al., Getting to 100%: six strategies for the challenging last 10%, Joule 6 (2022) 1981–1994.

[33] P. Denholm, D.J. Arent, S.F. Baldwin, et al., The challenges of achieving a 100% renewable electricity system in the United States, Joule 5 (2021) 1331–1352.

[34] H. Blanco, A. Faaij, A review at the role of storage in energy systems with a focus on power to gas and long-term storage, Renew. Sust. Energ. Rev. 81 (2018) 1049–1086.

[35] S. Sebastian, S. Wijewardane, S. Srinivasan, Recent advances in hydrogen production, storage, and fuel cell technologies with an emphasis on inventions, innovations, and commercialization, Solar Compass 8 (2023) 100065.

[36] T. Negash, A.A. Solomon, F. Ottermo, et al., System design issues of high renewable energy system, the case of Eritrea, Energy Policy 209 (2026), https://doi.org/10.1016/j.enpol.2025.114949. Epub ahead of print.

[37] M.G. Ghebrezgabher, A.K. Weldegabir, Estimating solar energy potential in Eritrea : a GIS-based approach, Renew. Energy Res. Appl. 3 (2022) 155–164.

[38] K. Rosen, R. Van Buskirk, K. Garbesi, Wind energy potential of coastal Eritrea: an analysis of sparse wind data, Sol. Energy 66 (1999) 201–213.

[39] T. Negash, E. Möllerström, F. Ottermo, An assessment of wind energy potential for the three topographic regions of Eritrea, Energies (Basel) 13 (2020), https://doi.org/10.3390/en13071846. Epub ahead of print.

[40] N. Teklebrhan, A.A. Solomon, F. Ottermo, et al., Strategies for integrating residential PV and wind energy in Eritrea's electricity grid by imposing feed-in constraints in low voltage network, Sol. Energy 286 (2025), https://doi.org/10.1016/j.solener.2024.113140. Epub ahead of print.

[41] K. Quizhpe, P. Arévalo, D. Ochoa-Correa, E. Villa-Ávila, Optimizing microgrid planning for renewable integration in power systems: a comprehensive review, Electronics 13 (18) (2024) 3620, https://doi.org/10.3390/electronics13183620.

[42] M.R. Shaner, S.J. Davis, N.S. Lewis, et al., Geophysical constraints on the reliability of solar and wind power in the United States, Energy Environ. Sci. 11 (2018) 914–925.

[43] A.W. Frazier, W. Cole, P. Denholm, et al., Storage Futures Study: Economic Potential of Diurnal Storage in the U.S. Power Sector, 2021. NREL/TP-6A20-77449.

[44] M. Nasser, T.F. Megahed, S. Ookawara, et al., Techno-economic assessment of clean hydrogen production and storage using hybrid renewable energy system of PV/wind under different climatic conditions, Sustain. Energy Techn. and Assess. 52 (2022) 102195.

[45] A. Zucker, T. Hinchliffe, Optimum sizing of PV-attached electricity storage according to power market signals – a case study for Germany and Italy, Appl. Energy 127 (2014) 141–155.

[47] D. Heide, M. Greiner, L. von Bremen, et al., Reduced storage and balancing needs in a fully renewable European power system with excess wind and solar power generation, Renew. Energy 36 (2011) 2515–2523.

[48] B.C. Ardenas, L. Swinfen-Styles, J. Rouse, et al., Energy storage capacity vs. renewable penetration: a study for the UK, Renew. Energy (2021), https://doi.org/10.1016/j.renene.2021.02.149. Epub ahead of print.

[49] O. Ruhnau, S. Qvist, Storage requirements in a 100% renewable electricity system: extreme events and inter-annual variability, Environ. Res. Lett. 17 (2022), https://doi.org/10.1088/1748-9326/ac4dc8. Epub ahead of print.

[50] B. Wang, B. Zhaoxiang, Hydrogen energy storage: mitigating variability in wind and solar power for grid stability in Australia, Int. J. Hydrog. Energy 97 (2025) 1249–1260.

[51] L. Li, J. Lin, N. Wu, et al., Review and outlook on the international renewable energy development, Energy Built Environ. 3 (2022) 139–157.

[52] R. Khakimov, A. Moskvin, O. Zhdaneev, Hydrogen as a key technology for long-term & seasonal energy storage applications, Int. J. Hydrog. Energy 68 (2024) 374–381.

[53] S. Weitemeyer, D. Kleinhans, T. Vogt, et al., Integration of renewable energy sources in future power systems: the role of storage, Renew. Energy 75 (2015) 14–20.